P2B.4 WIND TURBINE AND SODAR OBSERVATIONS OF WAKES IN A LARGE WIND FARM

Robert J. Conzemius*
WindLogics, Inc.
Grand Rapids, Minnesota, USA

1. INTRODUCTION

The minimization of wind turbine wake impacts is one of the primary considerations in wind farm design. Yet, due to the turbulent nature of wakes, they are often rather difficult to model, and the problem becomes particularly challenging when large arrays are planned, due to the potential for multiple interactions among wakes. The cumulative effects of upstream turbines can have a substantial impact on both wind farm output as well as site suitability.

Numerous models exist for characterizing wind turbine wakes (Barthalmie et al. 2006). Due to the great computational expense of explicitly simulating turbine wakes, these models employ great simplifications in order to make it possible to optimize the layout of large wind turbine arrays. This optimization involves calculating cumulative wake effects for a myriad of different possible configurations. Bartholmie et al. (2003, 2006) have tested these models at offshore wind farms, but validation at various onshore wind farms is rather limited.

In the present study, we have taken measurements of wind turbine wakes using a combination of sodar and wind turbine nacelle observations. To focus the evaluation specifically on atmospheric turbulence and its effects on turbine wakes and to avoid the complicating effects of topography, we have chosen for our study a wind farm located in relatively simple terrain. The wind farm provided supervisory control and data acquisition (SCADA) data on a turbine-by-turbine level every 10 minutes. We placed two sodar instruments in the farm with the intent of measuring both the free-stream (unwaked) air flow and the turbine wakes. The study is somewhat similar to one conducted by Elliott and Barnard (1990), in which wind turbine wakes were measured using meteorological towers placed in an operating wind farm over land. We seek to update that study using measurements from a more recently built farm with significantly larger wind turbines.

Wind tunnel measurements of wind turbine wakes (Chamorro and Porté-Agel 2009) have revealed counter-rotational effects of rotor torque. It remains to be seen whether these effects are present and measureable in operating wind farms. Thus, one goal of the present study is to analyze additional field measurements of wind turbine wakes in operating wind farms, where the measurements include the full scale of atmospheric turbulence, to assess any differences between the wind tunnel measurements and atmospheric observations.

Fig. 1. Layout of the southwestern portion of the wind farm and placement of the sodars.

2. EXPERIMENTAL SETUP

2.1. Wind farm location

The wind farm chosen for our observations is located in Mower County, Minnesota and is operated by NextEra Energy Resources, Inc. The farm contains 43 Siemens SWT2.3-93 turbines, each with a peak capacity of 2.3 MW, and has been operating since late 2007. In the summer and fall of 2009, we collected SCADA data from the farm. The SCADA data provide 10-minute averages of ambient atmospheric temperature and wind speed at the nacelle, power output, blade pitch angle, and rotor RPM. In general, the wind farm layout was designed to minimize wake impacts for the two prevailing wind directions at the site, which are from the northwest and from the south. For this reason, we focused our analysis on the southwestern portion of the farm (Fig. 1), where one wind turbine row is oriented more north to south than the others and is therefore more likely to experience turbine wake effects. Due to the fact that

measurement equipment could only be placed on turbine access roads within the farm, this southwestern segment was an ideal monitoring location because the row curves at a nearly 90-degree angle, making it possible to measure waked and unwaked wind profiles within this row simultaneously.

2.2. Sodar data

We placed two SecondWind Triton sodars within this wind turbine segment (see Fig. 1) in order to measure the unwaked and waked wind speed profiles. The first was placed midway between Turbines 39 (T39) and 40 (T40) with the intention of measuring the background atmospheric wind profile during periods when the wind is coming from the south, which is one of two prevailing wind directions for the site. The second sodar was placed between T41 and T42, but as close to T42 as possible, in order to measure downstream wake impacts from T41.

The sodars measure the vertical wind profile using three beams, each 10 degrees off the vertical, and separated horizontally by 120 degrees. The half power beam width is approximately 11 degrees. The Tritons are typically deployed so that one of the three beams points directly south. Pulses from each of these three beams are sent out at approximately 10 second intervals, and the return signals are averaged over a 10-minute period to calculate the vertical wind profile. The profile includes all three components of velocity at heights of 40, 50, 60, 80, 100, 120, 140, 160, 180, and 200 meters above ground level (AGL). Additionally, an estimate of turbulence intensity at each of these levels is included. A barometer is also contained within the unit as well as a thermometer at the 2-meter level on the outside edge of the dish so that air density can be calculated for each 10-minute observation. The sodars were deployed on July 31, 2009 and remained operating in the wind farm until December 14, 2009.

2.3 Data analysis technique

In the wind tunnel (Chamorro and Porte-Agel 2009), the turbulent and time-averaged components of velocity were measured using a fast-response hot wire probe that could be moved to any position relative to the wind turbine location, and the air flow and vertical temperature gradient within the tunnel could be precisely controlled. The measurements provided vertical cross-sections and profiles of mean wind and turbulence properties for neutral atmospheric conditions. In the wind farm, such control over the wind and temperature and measurement locations is not possible, so it is necessary to use a compositing technique to construct the wake vertical profiles and cross sections from all measurements available throughout the course of the field measurement campaign. It is possible to categorize the measurements in terms of Richardson number, nocturnal versus convective boundary layer conditions, or more simply in terms of the atmospheric temperature gradient. However, due to sampling size limitations, it was not possible to restrict the measurements to a precise set of conditions as was done in the wind tunnel. Therefore, some variation in conditions (for example, a composite formed using measurements with a similar vertical temperature gradient may have had different temperatures and different wind speeds) within any of the constructed composites was an undesired yet necessary result.

We used a cylindrical coordinate system for our analyses, with range (meters), azimuth (degrees), and height (meters above ground level) as the three coordinates and the zero azimuth pointed in the direction of the upwind turbine, which, in our presented analyses, is Turbine 41 (WT41—hereafter we shall denote wind turbines by the letters 'WT' followed by the turbine number). For the SCADA data, whose variables are all measured at 80 meters AGL, the analyses are presented as functions of azimuth only. Analyses based on sodar data are presented as a function of both azimuth and height above ground level.

In order to classify the data according to atmospheric stability, we calculated the vertical temperature gradient by taking the difference between the average of the nacelle ambient temperature measurements (from all 43 turbines) and the average of the two sodar temperatures and dividing by the 78 meter difference in height between those two levels. The vertical temperature gradient values in Table 1 were used as limits of our stability categories.

In order to focus on occurrences of more meaningful wake impacts, we eliminated any time periods when either the upstream or waked turbine was offline or when the wind speed was too light for both turbines to be producing at least 150 kW power. Likewise, if the wind speed was large enough for either turbine to reach the maximum power of 2300 kW (meaning that one or both turbines might be operating on the upper, flat part of the power curve), we eliminated that time period from the analysis.

The yaw angle of the "downstream" turbine was used as the wind direction for all measurements, and the compass direction terminology was used. Under such terminology, angles increase in the clockwise direction and decrease in the counterclockwise with zero degrees representing wind coming from due north (our analysis still defines zero angle as pointing toward the upstream turbine, however).

Prior to performing the calculations, we corrected the yaw angles from the SCADA data. The correction procedure was needed in order to remove yaw angle offsets that developed in the archiving system as a result of turbine downtime (for fault conditions, maintenance, or other reasons). When turbines are subsequently brought back online, the yaw angle is erroneously recorded as unchanged from its previous uptime value, even when the actual yaw angle has

changed. These errors appear to be a result of archival software design.

In order to construct vertically consistent sodar cross-sections and vertical profiles, we limited our analysis to times when the entire vertical profile was available. This occurred only 19% of the time, but the length of the data collection period allowed a sufficient number of measurements to be collected to form a composite cross section.

Table 1. Temperature Gradient Ranges Used for Stability Classification

Stability Class	Temperature Gradient (K/km)
A,B	<-1.7
C	-1.7<x<-1.5
D	-1.5<X<-0.55
E	-0.55<X<1.5
F	1.5<X<100

3. RESULTS

3.1 SCADA analysis

Due to the fluctuations in wind speed caused by background atmospheric boundary layer turbulence (this is particularly true in the convective boundary layer), wind turbine wakes may not be recognizable in SCADA data during individual instances of waking. Rather, the SCADA data reveal wakes when it is composited using all available measurements over the course of the field measurement campaign. We show the data by calculating the ratios of wind speed and power from the SCADA data from WT42 and WT41 in order to indicate the velocity deficit. Although a large amount of scatter is obvious in the plots (Fig. 2), if the data points are binned in five-degree increments (red lines), the wakes are more clearly seen in the data When WT42 is waked, the ratio of the WT42 to WT41 wind speeds drops below unity. When WT41 is waked and WT42 is unwaked, the ratio becomes larger than one. It is possible to see the evidence of waking from various pairs of turbines in the row. However, only neighboring turbines appear to have an impact on each other in these plots.

Due to the roughly cubic nature of the relationship between wind speed and power over the range of wind speeds considered, plots of power ratio as a function of wind direction (Fig. 2b) show larger peaks and valleys and also more scatter in the ratio, but overall, the power data confirm the relationships among turbines shown by the wind speed data.

Atmospheric stability plays a large role in the scatter of the data points due to its impact on background atmospheric turbulence (Fig. 3). When the background atmospheric temperature profile is unstable (Fig. 3a), there is considerably larger scatter in the power ratio, making it difficult to detect the wake impacts, even when the data are binned. The results are strongly indicative of the role of atmospheric turbulence in bringing about the breakup of turbine wakes during unstable conditions, when the production of atmospheric turbulence due to buoyancy effects is rather pronounced. On the opposite end of the stability scale (Fig. 3b), wake impacts are more pronounced, relative to the background scatter, when the atmospheric temperature profile is very stable and background atmospheric turbulence is either suppressed or its length scales reduced. In either case, the impact of atmospheric turbulence on turbine wakes is much less, and they persist farther downstream.

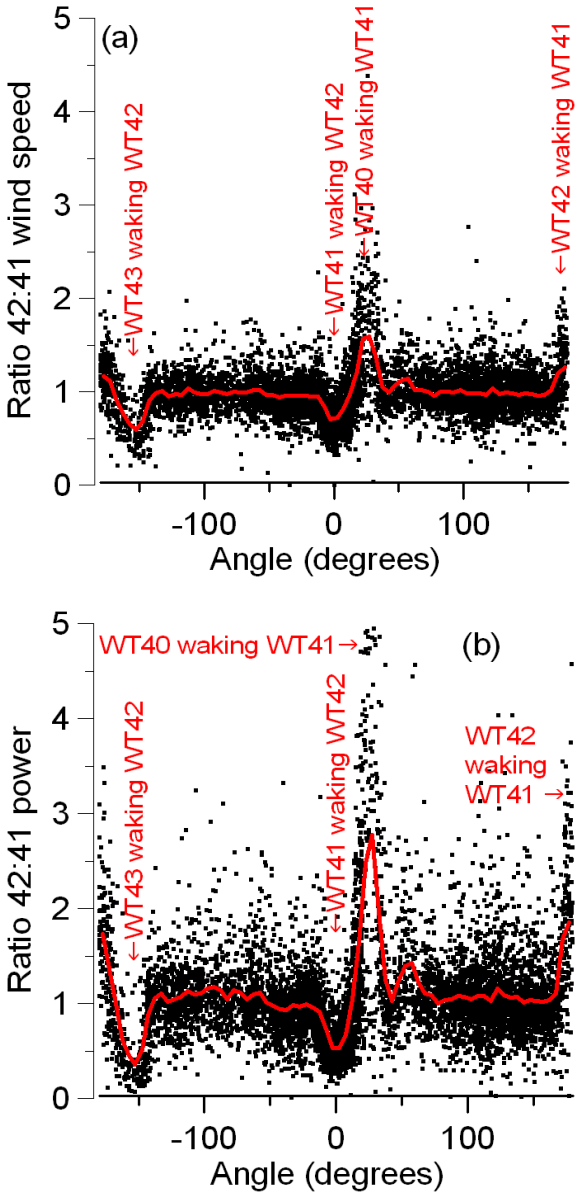

Fig. 2. Ratio of WT42 to WT41 SCADA variables: (a) wind speed, and (b) active power. The red lines denote averages of observations in 5-degree bins.

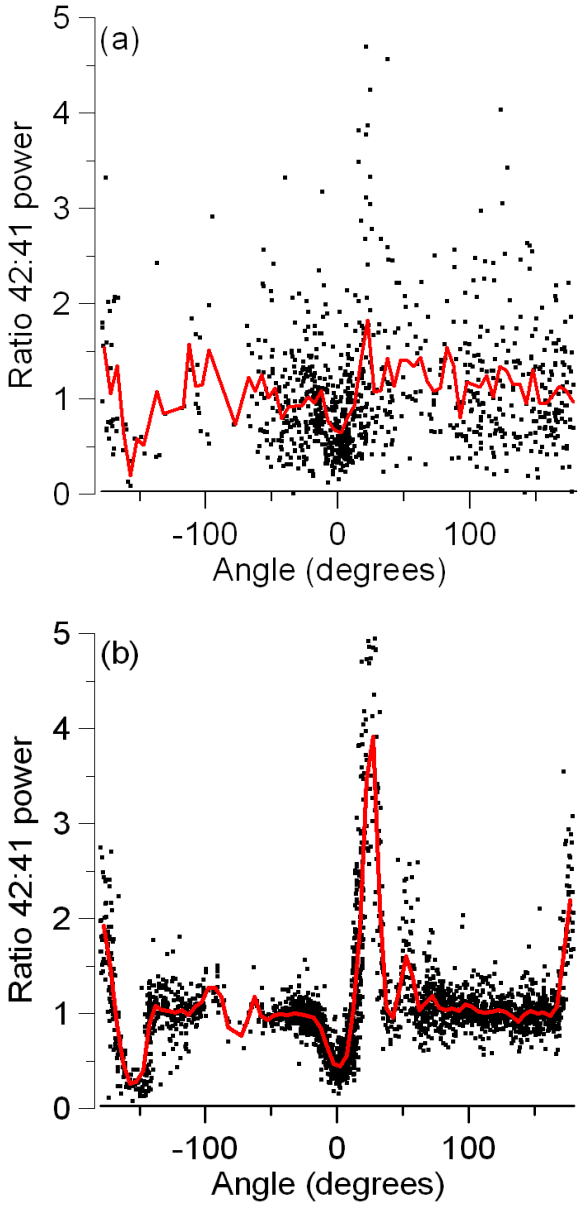

Fig. 3. Ratio of WT42:WT41 power as a function of atmospheric stability (see Table 1): (a) class A/B, and (b) class F. The red lines denote averages of observations in 5-degree bins.

3.2. Sodar data

Sodar composite cross-sections can reveal the effects of multiple atmospheric processes on the turbine wakes. One question about the wake measurements is whether or not rotational effects exist in the wake, and if so, whether they can be detected by sodar. The cross sections of vertical velocity (Fig. 4) suggest that the sodars have measured rotation of the turbine wake during the experiment. Positive vertical velocity is preferentially located to the left of the wake centerline, and negative vertical velocity is oriented more to the right, with the zero isotach slanting downward from left to right across the wake. Although this configuration may not be purely rotational (in particular, positive vertical velocity tends to be found at low levels under the entire wake), the sign of rotation matches that which would be expected for the blade rotation of the SWT2.3-93 turbines.

An additional aspect of the wake is that it appears sheared and rather oval-shaped, with the long axis of the oval oriented from the upper left to lower right. This effect is due to the wind shear that is most often present during nocturnal or stable conditions, when the wakes are most persistent and easily detectable. During such conditions, the wind vectors point more to the left at very low altitudes and more to the right above (when seen in the framework moving with the flow), due to the balance of vertical turbulent momentum exchange (Reynolds stresses) and the Coriolis and pressure gradient forces. This sort of a vertical profile is consistent with the Ekman profile: if the horizontal component of the velocity vectors were plotted on a Cartesian axis, a spiral shape would result.

Perhaps the most noticeable characteristic of the wake is the offset of minimum velocity deficits to the left of the so-called centerline at Y/Rd=0. We hypothesize that the positive vertical velocity may advect smaller wind speeds from lower altitudes. Alternatively, the effects of wind shear may simply move the deficit, which can generally be expected to occur just above the hub height, to the left. Note that the reference wind speed is taken from the 80 meter level.

The wake recovery as a function of distance can be estimated using all of the available data from the two operating sodars in the farm. Figure 5 shows the wind speed ratios of the sodars as a function of wind direction. In this case, zero degrees is oriented to the north. This plot, which we refer to as a “sodar rose”, reveals distinct wakes whose impacts can be roughly quantified by taking the minimum of velocity ratio along a 30-degree arc centered on the azimuth pointing to the turbine causing the wake. Although there are more turbines in the row than are indicated in the sodar rose, not all of them have a discrete wake impact. In those cases, the turbine may be too far away for the sodar to consistently measure its wake, or the wake may be too close to the wake of another turbine to be measured as a distinct wake. For example, WT39 appears to have no impact on Triton169 because the sodar wind speed ratio is almost exactly unity in the direction from Triton169 to WT39.

Taking into account all the wake information from the sodar rose, as well as the distances between the sodars and the respective turbines, one can estimate the wake as a function of distance (Fig. 6). In general, the curve that can be inferred is that of a negative exponential function that asymptotically approaches unity.

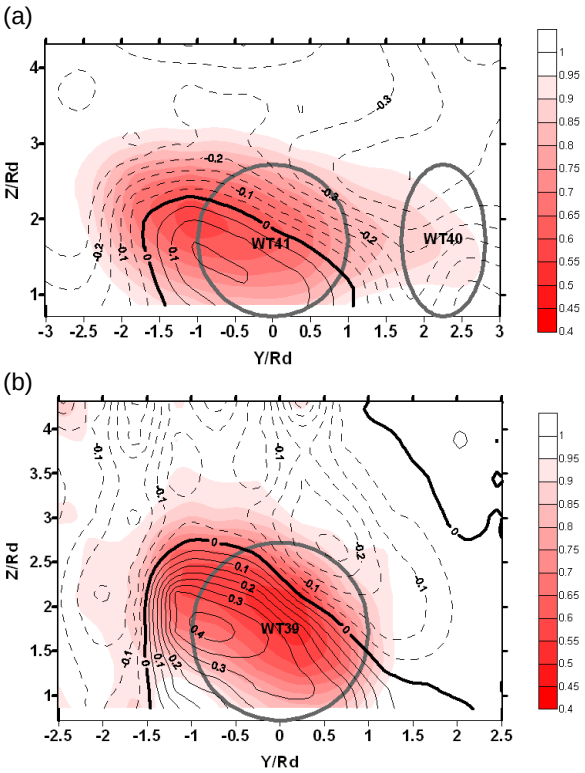

Fig. 4. Cross sections of waked:unwaked wind speed ratio (shading) and vertical velocity (black lines—dashed lines are negative, contour interval of 0.05 m/s) for the following pairs of turbines: (a) WT42 (waked) and WT41 (unwaked), and (b) WT40 (waked) and WT39 (unwaked). The rotor diameter of each turbine responsible for a velocity deficit is shown with a solid gray line.

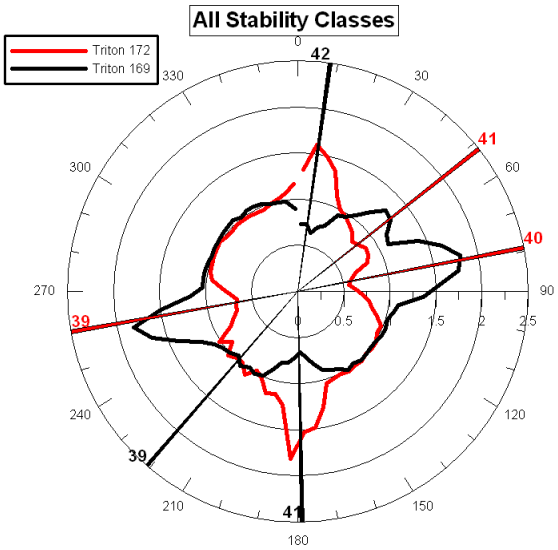

Fig. 5. Wind speed ratios of the two sodars computed by averaging all observations in 5-degree bins. The red line denotes the ratio Triton172:Triton169, and the black line denotes its inverse. The radials indicate the direction towards turbines responsible for the measured wakes and are colored according to the sodar that is measuring the wake (red for Triton 172; black for Triton 169).

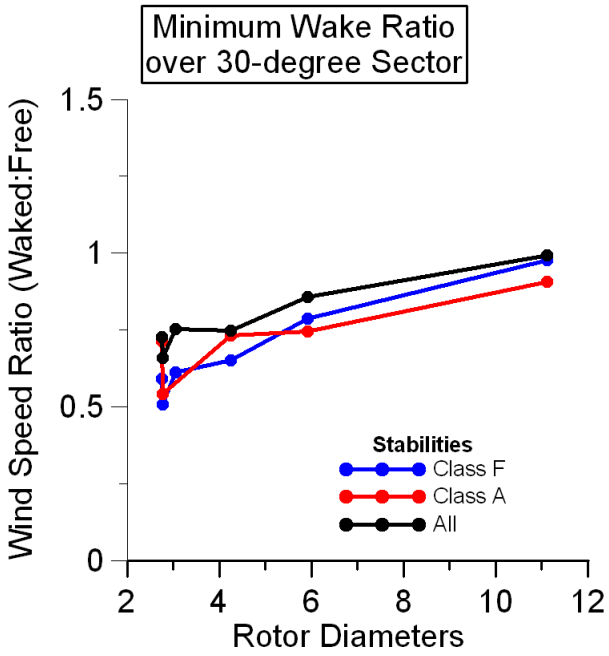

Fig. 6. Wind speed ratio as a function of distance for the wakes indicated in Fig. 5, taken as the minimum of the ratio in a 30-degree arc centered on each turbine direction. The black line indicates the ratio for all observations, the red line indicates class A/B stabilities, and the blue line indicates class F.

We made an attempt to categorize the wake recovery according to atmospheric stability, but the results do not have the expected stratification. One would expect a slower wake recovery with stronger stability, but either the atmospheric stability is not having such an effect on the wakes, or the field experiment collected an insufficient number of samples to clearly see the relationships that exist between atmospheric stability and turbine wake recovery. We believe the latter of these two possibilities to be true. In either case, approximately 80 percent wake recovery has occurred by 12 rotor diameters downstream, with speed ratios there increasing to 0.9 from a minimum of 0.5 at a distance of 3 rotor diameters downstream.

3.3 Cumulative wake impacts

Finally, we examine the cumulative wake impacts of multiple turbines in a row. We oriented the SCADA analyses for WT33 through WT38 so that the zero azimuth was pointed at WT32. As is demonstrated in the analysis (Fig. 7), the accumulation of wakes causes the velocity deficit to grow in width and depth proceeding down the row of turbines. We averaged the wind power ratio (WTXX:WT32) over a 30-degree width centered on zero degrees for each of these turbines, and the results are presented in Fig. 8. We have also separated the results into the various atmospheric stability categories. In general, the wake accumulation is more severe for more stable

conditions, which favor the persistence of wakes. In unstable conditions, greater atmospheric turbulence favors the rapid breakup of wakes. Nevertheless, significant wake accumulation occurs in all of the stability categories.

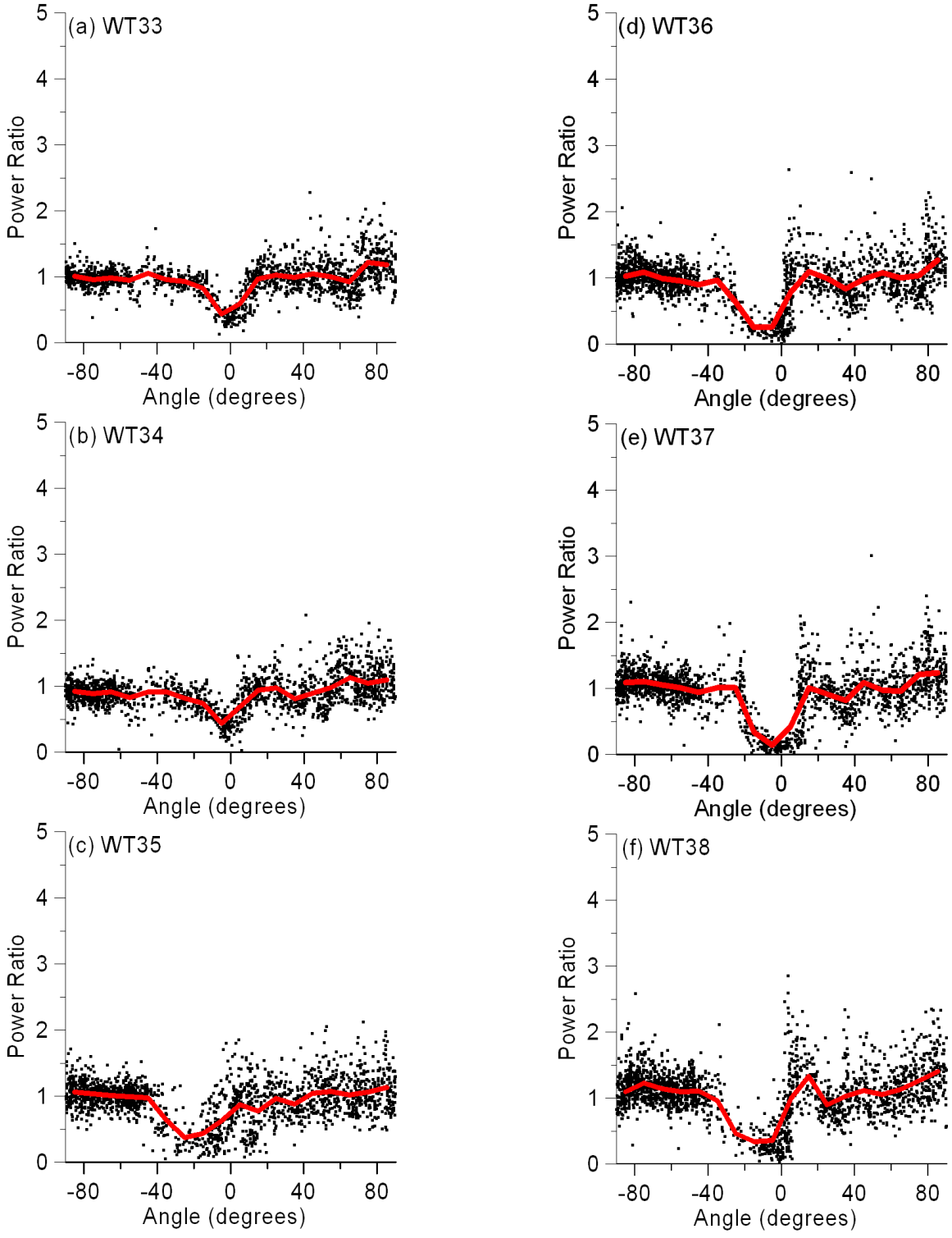

Fig. 7. Ratio of the power output of the selected turbine to the power output of WT32 during all occurrences of F class stability: (a) WT33, (b) WT34, (c) WT35, (d) WT36, (e) WT37, and (f) WT38. The red lines denote the average of data points in five-degree bins.

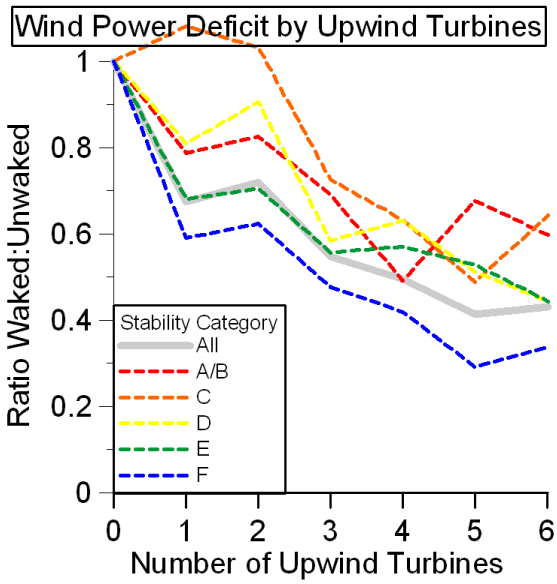

Fig 8. Power ratio of waked:unwaked turbines as a function of the number of upwind turbines in the WT32 to WT38 row for all observations in the dataset (solid gray line) and separated according to stability category (dashed colored lines).

4. SUMMARY AND FUTURE WORK

The SCADA data show that wakes can be measured on land when the data are composited. However, atmospheric turbulence plays a large role in determining how persistent and detectable those wakes are. In unstable conditions, which are characterized by buoyancy-produced turbulence, a deep convective boundary layer forms with large, organized structures on the order of 1 km in size. This turbulence causes meandering and rapid destruction of wind turbine wakes. In these conditions, the composited SCADA data show only a relatively subtle wake signature.

In stable conditions, turbulence is of a smaller length scale and relatively suppressed. Turbine wakes in those conditions are much more persistent and are well-visualized in the SCADA data.

Cross sections prepared from composite SODAR data, show the effects of multiple atmospheric processes on the wakes. Some wake rotation is evident and matches the counter-rotation that would be expected from the rotation of the turbine blades. The oval shape of the wake reflects wind shear that occurs during stable atmospheric conditions. Additionally, the greatest velocity deficit is shifted up and to the left when viewed from a perspective looking upstream at the turbine generating the wake. This displacement could be due either to the shear or to the upward advection of slower velocity by the upward component of the turbine rotation. SODAR data also have been used to demonstrate the recovery of wakes and show that by about 12 rotor diameters downstream, at least 80 percent recovery has occurred.

The effect of accumulated wakes has been measured by SCADA data from a turbine row within the farm. The accumulation of velocity deficit in the combined wakes is most significant during the most stable atmospheric conditions. The wake accumulation is manifested in both the width and the minimum of the velocity deficit within the wake.

ACKNOWLEDGEMENTS.

This research was supported by customers of Xcel Energy through a grant (RD3-42) from the Renewable Development Fund, and the University of Minnesota Institute for Renewable Energy and the Environment. Drs. Fotis Sotiropoulos and Fernando Porte-Agel of the University of Minnesota, Saint Anthony Falls Laboratory were instrumental in securing this grant. Barr Engineering Company assisted with the deployment of SODARS.

REFERENCES

Barthelmie, R. J., L. Folkerts, F. T. Ormel, P. Sanderhoff, P. J. Eecen, O. Stobbe, and N. M. Nielsen, 2003: Offshore wind turbine wakes measured by sodar. *J. Atmos. and Oceanic Technol.,* **20,** 466-477.

Barthelmie, R. J., L. Folkerts, G. C. Larsen, K. Rados, S. C. Pryor, S. T. Frandsen, B. Lange, and G. Schepers, 2006: Comparison of wake model simulations with offshore wind turbine wake profiles measured by sodar. *J. Atmos. and Oceanic Technol.,* **23,** 888-901.

Chamorro, L. P. and F. Porte-Agel, 2009: A wind tunnel investigation of turbine wakes: boundary layer turbulence effects. *Boundary Layer Meteorol.,* **132,** 129-149.

Elliott, D. L., and J. C. Barnard, 1990: Observations of wind turbine wakes and surface roughness effects on wind flow variability. *Solar Energy,* **45,** 265-283.